Chapter 1

Introduction

This chapter contains a brief history and overview of celestial mechanics from the beginning of seventeenth century to the present year. During this period, there has been a tremendous advancement in works related to the dynamics of two and three bodies. Studies on periodic, quasi–periodic and chaotic motion of a body in the restricted three–body problem and stability, resonance phenomena, effect of solar radiation pressure and oblateness of the primaries are reviewed. The development of the equations of motion and the methodology used for the generation of Poincaré surface of sections are also presented.

1.1   Historical survey

Mechanics deals with the behavior of physical bodies under the effect of forces. Celestial mechanics is the branch of astronomy that deals with motion of celestial objects. In celestial mechanics, one applies the principles of mechanics to astronomical objects, such as stars and planets to produce ephemeris data. Orbital mechanics, a sub–field of celestial mechanics, deals with the orbits of planets and satellites.

Modern analytical celestial mechanics started with the publication of Newton's ***Philosophiae Naturalis Principia Mathematica*** in the year 1687. Over a century after Newton, Pierre Simon Laplace introduced the term ***Celestial Mechanics***. Johannes Kepler(1571–1630) was the one to introduce predictive geometrical astronomy. Prior to Kepler there was little connection between exact quantitative

prediction of planetary positions, using geometrical or arithmetical techniques.

Kepler enunciated his three laws of planetary motion during 1609 – 1619. These laws laid the foundation for the beginning of modern celestial mechanics. Kepler's three laws of planetary motion are

1. The orbit of each planet is an ellipse with the Sun located at one focus.

2. The radius vector of each planet sweeps out equal areas in equal time.

3. The square of the orbital period of a planet is proportional to the cube of its semi–major axis.

Kepler's laws of planetary motion led Newton to conclude that the force which keeps a planet in its orbit around the Sun varies inversely as the square of the distance between the Sun and the planet. Most of the results in celestial mechanics are obtained by treating the bodies as point masses. Such an assumption is justifiable mainly because of two reasons. Firstly, all members of solar system are separated by large distances and the dimension of the bodies is negligible compared to their separating distance. Secondly, all bodies can be assumed as spheres in the first approximation.

The gravitational attraction between two spherical bodies is, according to Newton's law of Gravitation, equal to the gravitational attraction between two point masses located at the respective centres of the two spherical bodies, each endowed with the mass of the body it represents. Thus, the problem of studying the gravitational force between two spherical bodies reduces to the study of motion of two points under the effect of their gravitational force. This problem is called the classical two–body problem. It was first solved by Newton by geometrical method and analytic solution was given by Bernoulli which was further investigated by Euler. The solution of two–body problem marks the starting point of celestial mechanics.

1.1.1 The three–body problem

In celestial mechanics, a two–body problem describes the motion of two rigid point masses orbiting about each other under the influence of their mutual gravitational

attraction. Satellites orbiting a planet, a planet orbiting a star or binary stars orbiting about their common centre of mass are examples of two–body problem.

A number of researchers tried to extend Newton's analytical method of solving two–body problem to three–body problem like Sun–Earth–Moon system. But the three–body problem, where the masses of all three bodies are arbitrary and are attracting each other according to Newtonian law and free to move in space with any initial conditions of motion, can not be solved analytically.

In the solar system, there are many bodies like natural satellites, asteroids and comets having negligible mass in comparison of planets and stars. Also, motion of planets around Sun is approximately circular. These facts suggested the concept of restricted three–body problem. In addition, it is one of the simplest non-integrable dynamical systems. This problem describes the motion of secondary body which moves under the gravitational effect of two finite masses called primaries. The primaries are supposed to move in circular orbits around their center of mass (barycenter) on account of their mutual attraction and the secondary body not influencing the motion of the primaries. It is known as circular restricted three–body problem (CRTBP). If primaries move in elliptical orbits then the problem is known as elliptical restricted three–body problem (ERTBP).

The restricted problem has important roles in space dynamics, celestial dynamics and analytical dynamics and in studying the motion of artificial satellites, natural satellites, planets, minor planets, and comets. For designing space missions, where a spacecraft is moving from Earth to Moon or between two planets, the RTBP could be applied. Problems related to space missions require analytical and numerical techniques to solve the circular or elliptical RTBP. In recent years, after the launching of artificial satellites in the Earth–Moon system and in the solar system, the applications of RTBP has gained considerable momentum in celestial mechanics.

The RTBP has been used first time to analyze lunar theories in 1772 by Euler and subsequently by [Lagrange (1772)]. They found five stationary points known as Lagrange points. The contributions of Euler, Jacobi and Poincaré [Poincare (1892)] are the most significant from the point of view of space mechanics applications. Many more mathematicians and astronomers have used the theory of RTBP [Hill(1878), Brunini (1996)],[Poincare (1892), Levi–Civita (1904)] and [Birkoff

(1915)] in modelling different systems. Using synodic(rotating) coordinate system, Jacobi evaluated a first integral of equations of motion known as the Jacobi integral. Jacobi integral connects magnitude of velocity vector and location of secondary body. Using this some qualitative behaviour regarding the problem can be determined without actually solving the equations of motion. [Hill(1878)] applied it first time to celestial mechanics for describing the motion of the Moon. He proved that distance between Earth and Moon is always bounded. To prove this [Hill(1878)] used the Jacobi integral. After that Brown in 1896 gave the most precise lunar theory.

[Pars (1965)] and [Pollard (1966)] have explained dynamics and mathematics in their books. **Theory of orbits** by [Szebehely (1967)] is an outstanding treatise on the restricted problem of three–bodies. [Moulton (1914), Plummer (1918), Winter (1941), Finlay–Freundlich (1958), Brouwer and Clemence (1961), Danby (1962), Mc Cuskey (1963), Duboshin (1978)] and [Siegel and Moser (1971)] have given detailed explanation of dynamics of RTBP.

1.1.2   Effect of solar radiation pressure

Photo–gravitational RTBP describes the motion of secondary body under the effect of mutual gravitational force of primaries as well as radiation pressure from one or both primaries. The Sun–Planet–Satellite system can be analyzed by considering the Sun as a radiating body, while Star–Star–Planet system can be analyzed by considering radiation pressure of both primaries.

The minute pressure exerted by radiation on bodies is inversely proportional to the square of the distance between the light source and the illuminated body. This law is experimentally demonstrated and stated by Lebedev in 1891. Since then many researchers have incorporated this perturbing force as well as other perturbing forces like oblateness, atmospheric drag etc. in the study of RTBP. The effect of the radiation force is complicated as it depends on particular geometry, physical and physicochemical characteristics of secondary body [Poynting (1904)] and [Robertson (1937)]. It has been found that radiation force produces non–negligible effects on the dynamics of the secondary body. Some of the noticeable contributions in the photo–gravitational RTBP are by [Radzievskii (1950), Chernikov

(1970), Kunitsyn and Perezhogin (1978), Bhatnagar and Chawla (1979), schuerman (1980), Choudhary (1985), Kunitsyn and Tureshbaev (1985), Kumar and Choudhary (1987), Sharma and Ishwar (1987), Lukyanov (1988), Ragos and Zagouras (1988), Ragos and Zagouras (1993), Markellos et. al. (1993), Kalantonis et. al. (2006), Papadakis (2006), Abdul Raheem and Singh (2006), Kalvouridis et. al. (2007), Namboodiri et. al. (2008), Das et. al. (2009a)] and [Das et. al. (2009b)].

The radiation force exerted by radiating primary on secondary body, can be divided into three components, namely, the radiation pressure, the Doppler shift of the incident radiation and the Poynting drag. The first two components act radially and the third component acts opposite to the velocity vector. [Poynting (1904), Robertson (1937)] have analyzed the latter two components, which are caused by the absorption and subsequent re–emission of radiation and constitute the Poynting–Robertson effect. Out of these three components of radiation force, the radiation pressure is the only significant component. The effect of Doppler shift of the incident radiation and the Poynting drag is negligible on the dynamics of secondary body [Radzievskii (1950)]. Solar radiation pressure force F_p changes with the distance by the same law as the gravitational attraction force F_g in opposite direction. According to [Kalvouridis et. al. (2007)] the resultant force exerted by the Sun on secondary body is given by,

$$F = F_g - F_p, \tag{1.1.1}$$

which can be expressed as

$$F = qF_g, \tag{1.1.2}$$

where,

$$q = 1 - \frac{F_p}{F_g}. \tag{1.1.3}$$

The effect of radiation pressure of the radiating primary on secondary body is expressed by means of the mass reduction factor

$$q = 1 - \varepsilon, \tag{1.1.4}$$

where the radiation coefficient ε, is the ratio of the force F_p which is caused by

radiation to the force F_g which results from gravitation; That is

$$\varepsilon = \frac{F_p}{F_g}. \tag{1.1.5}$$

This coefficient ε depends on the physical properties of the radiating primary, as well as those of the secondary body and is expressed by the formula given by

$$\varepsilon = \frac{3L}{16\mu cGM\rho s}, \tag{1.1.6}$$

where G is the gravitational constant. Mass and luminosity of the Sun are denoted by M and L respectively. [Lukyanov (1988)] found that luminosity of the Sun depends on the absolute temperature of the Sun. The mass and uniform density of the secondary body are denoted by s and ρ respectively. ε for given secondary body of radius a and uniform density ρ can be evaluated by knowing the mass and the luminosity of the Sun. If perturbing force due to radiation pressure is absent, it means $F_p = 0$, then $q = 1$. If $F_p > F_g$ then $\varepsilon > 1$, it means $q < 0$. If $F_p < F_g$ then $\varepsilon < 1$, it means $0 < q < 1$. The latter case is applied when we study photo–gravitational RTBP in the solar system.

1.1.3 Effect of oblateness

In classical RTBP, all the three bodies under consideration are taken as point masses. Such idealistic considerations are coming from the assumption that celestial bodies can be considered as spheres. From a physical point of view, it is unbelievable to take into account the celestial objects as perfect spherical bodies. Celestial objects will suffer from deformation in its shapes at poles due to the effect of rotation. For this reason, the oblate spheroid bodies are a good approximation for most of the celestial objects. RTBP incorporating oblateness of participating bodies have been considered by [Markellos et. al. (1996)], [Abouelmagd and Sharaf (2013)], [Abouelmagd et al.(2014)] and [Abouelmagd et. al. (2015)]. Oblateness is one of the main perturbations we should include when we consider such objects. The main perturbation forces experienced by the secondary body near Earth are the forces due to Earth's oblateness and pressure due to solar radiation apart from the gravitational force of the Sun and Earth.

For communication satellites which are located very near to Earth, oblateness of Earth is the main perturbating force. To study the dynamics of asteroid near Jupiter, effect of oblateness of the Jupiter is non–negligible. [Brouwer and Clemence (1961)], [Laplace (1805)], [Greenberg (1974)] and [Tisserand (1896)] have studied the motion of satellites of Saturn by incorporating perturbation due to oblateness of Saturn.

1.2 Potential due to oblate spheroid

The motion of secondary body has been investigated by making different assumptions on the nature and shape of the primaries. They are

1. when more massive body is oblate,

2. when more massive body is source of radiation and second primary is an oblate spheroid, and

3. when more massive body is source of radiation and both primaries are oblate.

In all the above three cases the motion of secondary body is affected due to perturbation. We have studied the photo–gravitational circular restricted three–body problem in which the infinitesimal body moves under the gravitational effect of the primaries, which orbit around a common centre of mass in circular orbits. For example, the Sun is a source of radiation and is almost spherical, while some of the planets are oblate. Two primary bodies revolve around their center of mass in circular orbits in a plane, coinciding with equatorial plane, under the influence of their mutual gravitational attraction. The third body, called the secondary body, moves in the plane of primaries under the gravitational effect of the primaries.

We assume that second primary is oblate spheroid. We use A_2 to represent oblateness coefficient of the smaller primary. Thus,

$$A_2 = J_2 R^2, \tag{1.2.1}$$

where J_2 is the dimensionless coefficient that characterizes the size of non spherical components of the potential with respect to smaller primary. R is the mean radius of the body.

If the object has axial symmetry, it can be shown from potential theory that the gravitational potential experienced by the third body can be written as [Murray and Dermot (1999)]

$$V = -\frac{Gm_0}{r}\left[1 - \sum_{n=2}^{\infty} J_n\left(\frac{R_0}{r}\right)^n P_n(\sin\delta)\right]. \tag{1.2.2}$$

where G is the universal gravitational constant, m_0 and R_0 are the mass and the mean radius of the object, respectively. δ denotes the latitude of the satellite, $P_n(\sin\delta)$ are Legendre polynomials of degree n, r is the distance from the centre of the object to satellite and J_n is the dimensionless coefficient that characterizes the size of non spherical components of the potential.

1.3   The mean motion

In orbital mechanics, the mean motion, denoted by n, refers to the angular speed required by the body to make one complete orbit. If τ denotes the orbital period, then the mean motion is given by $n = 2\pi/\tau$. To obtain the effect of oblateness on the mean motion, we shall proceed as follows. If the motion of two objects is in the same plane $(\delta = 0)$ then (1.2.2) becomes,

$$V = -\frac{Gm_0}{r}\left[1 - \sum_{n=2}^{\infty} J_n(\frac{R_0}{r})^n P_n(\sin 0)\right], \tag{1.3.1}$$

where,

$$P_{2n}(0) = \frac{(-1)^n(2n)!}{2^{2n}(n!)^2}, \tag{1.3.2}$$

and

$$P_{2n+1}(0) = 0. \tag{1.3.3}$$

For the first zonal harmonic, equation (1.3.1)can be reduced to,

$$V = -Gm_0\left[\frac{1}{r} + \frac{J_2 R_0^2}{2r^3}\right]. \tag{1.3.4}$$

Now assume that m_1, m_2 and m are the masses of the bigger, smaller and infinitesimal bodies, r_1 and r_2 are the distance of the m from m_1 and m_2, respectively. Let m_1 and m_2 have circular orbits about their common centre of mass and m is moving

under their gravitational influence in the same plane but it is so small that it does not affect their motion. Let

$$\vec{r} = u\hat{i} + v\hat{j} \tag{1.3.5}$$

be the position vector of m_2 with respect to m_1, r is the separation distance between m_1 and m_2. Using equation (1.3.1), the potential V_{12} between m_1 and m_2 can be written as

$$V_{12} = -Gm_1m_2\left[\frac{1}{r} + \frac{A_2}{2r^3}\right], \tag{1.3.6}$$

where,

$$A_2 = J_2R_0^2. \tag{1.3.7}$$

The equation of motion of m_2 with respect to m_1 can be written as

$$\ddot{\vec{r}} = -\frac{m_1 + m_2}{m_1m_2}\nabla V_{12}, \tag{1.3.8}$$

where,

$$\nabla = \frac{\partial}{\partial u}\hat{i} + \frac{\partial}{\partial v}\hat{j}. \tag{1.3.9}$$

Taking $u = r\cos nt$ and $v = r\sin nt$ in equation (1.3.5) and differentiating twice, we get

$$\ddot{\vec{r}} = -n^2\vec{r}. \tag{1.3.10}$$

Further, we have

$$\nabla V_{12} = \left(Gm_1m_2\left[\frac{1}{r^3} + \frac{3}{2}\frac{A_2}{r^5}\right]\right)\vec{r}. \tag{1.3.11}$$

Now using equations (1.3.10) and (1.3.11) in equation (1.3.8), we get the expression for mean motion as

$$n^2 = G(m_1 + m_2)\left[\frac{1}{r^3} + \frac{3}{2}\frac{A_2}{r^5}\right]. \tag{1.3.12}$$

For a spherical body, $A_2 = 0$, and hence we get $n^2 = \dfrac{G(m_1 + m_2)}{r^3}$.

1.4 Equations of motion with perturbation due to solar radiation and oblateness

Consider the RTBP in which the bigger primary of mass m_1 is a source of radiation and the smaller primary of mass m_2 is an oblate spheroid. To obtain the equations of motion for the secondary body, we choose the origin O as the centre of mass of the two primaries. We choose XY as the sidereal frame xy as the synodic frame such that O serves as the origin for both systems. We also choose the synodic frame to rotate with angular velocity n in the positive direction. Let the co-ordinates of m_1, m_2 and m in the sidereal frame be (X_1, Y_1), (X_2, Y_2) and (X, Y), respectively, and that in the synodic frame be (x_1, y_1), (x_2, y_2) and (x, y), respectively.

The transformation from synodic system (x, y) to inertial sidereal system (X, Y) is given by

$$\begin{pmatrix} X \\ Y \end{pmatrix} = \begin{pmatrix} \cos nt & -\sin nt \\ \sin nt & \cos nt \end{pmatrix} \begin{pmatrix} x \\ y \end{pmatrix}, \tag{1.4.1}$$

where,

$$\begin{pmatrix} \cos nt & -\sin nt \\ \sin nt & \cos nt \end{pmatrix}$$

is a transformation matrix. The equations of motion for the secondary body in the inertial sidereal frame, using Newton's law, are

$$m\ddot{X} = -\frac{\partial V}{\partial X}, \tag{1.4.2}$$

and

$$m\ddot{Y} = -\frac{\partial V}{\partial Y}. \tag{1.4.3}$$

Here $V = V_1 + V_2$, where V_1, V_2 denote the gravitational potential due to the masses m_1 and m_2. Since the first primary is radiating and the second primary is oblate spheroid, we express V in the form

$$V = -Gmm_1 \left[\frac{q}{r_1} \right] - Gmm_2 \left[\frac{1}{r_2} + \frac{A_2}{2r_2^3} \right]. \tag{1.4.4}$$

Adopting the terminology of [Szebehely (1967)], we choose $r = 1$ and the unit of

mass is chosen such that $\mu = 1$. This implies that $Gm_1 = (1 - \mu)$ and $Gm_2 = \mu$. The coordinates of masses m_1 and m_2 are taken as, $(x_1, y_1) = (\mu, 0)$ and $(x_2, y_2) = (\mu - 1, 0)$, respectively.

The velocity and acceleration components are given, respectively, by

$$\begin{pmatrix} \dot{X} \\ \dot{Y} \end{pmatrix} = \begin{pmatrix} \cos nt & -\sin nt \\ \sin nt & \cos nt \end{pmatrix} \begin{pmatrix} \dot{x} - ny \\ \dot{y} + nx \end{pmatrix}, \tag{1.4.5}$$

and

$$\begin{pmatrix} \ddot{X} \\ \ddot{Y} \end{pmatrix} = \begin{pmatrix} \cos nt & -\sin nt \\ \sin nt & \cos nt \end{pmatrix} \begin{pmatrix} \ddot{x} - 2n\dot{y} - n^2 x \\ \ddot{y} + 2n\dot{x} - n^2 y \end{pmatrix}. \tag{1.4.6}$$

Equations (1.4.2) and (1.4.4) now takes the form

$$\ddot{X} = -\frac{\partial}{\partial X} \left[-(1 - \mu) \left[\frac{q}{r_1} \right] - \mu \left[\frac{1}{r_2} + \frac{A_2}{2r_2^3} \right] \right], \tag{1.4.7}$$

where

$$r_1^2 = (X - X_1)^2 + (Y - Y_1)^2, \tag{1.4.8}$$

and

$$r_2^2 = (X - X_2)^2 + (Y - Y_2)^2. \tag{1.4.9}$$

Using equations (1.4.8), (1.4.9) in (1.4.7) and equating with (1.4.6), we get

$$\begin{aligned}
&\left(\ddot{x} - 2n\dot{y} - n^2 x \right) \cos nt - \left(\ddot{y} + 2n\dot{x} - n^2 y \right) \sin nt \\
&= -(1 - \mu) \frac{q}{r_1^3} \left[[(x - \mu) \cos nt - y \sin nt] \right. \\
&\left. - \mu \left[\frac{1}{r_2^3} + \frac{3A_2}{2r_2^5} \right] [(x - \mu + 1) \cos nt - (y) \sin nt] \right].
\end{aligned} \tag{1.4.10}$$

Similarly by using (1.4.3), we can arrive at

$$\begin{aligned}
&\left(\ddot{x} - 2n\dot{y} - n^2 x \right) \sin nt + \left(\ddot{y} + 2n\dot{x} - n^2 y \right) \cos nt \\
&= -(1 - \mu) \frac{q}{r_1^3} \left[(x - \mu) \sin nt + y \cos nt \right] - \mu \left[\frac{1}{r_2^3} + \frac{3A_2}{2r_2^5} \right] [(x - \mu + 1) \sin nt + (y) \cos nt].
\end{aligned} \tag{1.4.11}$$

Equations (1.4.10) and (1.4.11) can, respectively, be couched in the form

$$\ddot{x} - 2n\dot{y} = \frac{\partial \Omega}{\partial x}, \tag{1.4.12}$$

$$\ddot{y} + 2n\dot{x} = \frac{\partial \Omega}{\partial y}, \tag{1.4.13}$$

where,

$$\Omega = \frac{n^2}{2}\left[(1-\mu)r_1^2 + \mu r_2^2\right] + \frac{q(1-\mu)}{r_1} + \frac{\mu}{r_2} + \frac{\mu A_2}{2r_2^3}. \tag{1.4.14}$$

Here,

$$r_1^2 = (x-\mu)^2 + y^2, \tag{1.4.15}$$

and

$$r_2^2 = (x+1-\mu)^2 + y^2. \tag{1.4.16}$$

The mean motion n, the mass reduction factor q and the oblateness coefficient A_2 are respectively given by

$$n^2 = 1 + \frac{3}{2}A_2, \tag{1.4.17}$$

$$q = 1 - \frac{F_p}{F_g}, \tag{1.4.18}$$

$$A_2 = \frac{R_e^2 - R_p^2}{5R^2}, \tag{1.4.19}$$

where F_g and F_p represent the gravitational and radiation pressure forces, respectively. R_e and R_p denote the equatorial and polar radii of second primary, respectively, and R is the distance between primaries.

The system of equations (1.4.12)and (1.4.13) together with equation (1.4.14) admits a first integral in the form

$$\dot{x}^2 + \dot{y}^2 = 2\Omega - C, \tag{1.4.20}$$

where the constant of integration C is known as the Jacobi constant and is given by

$$C = n^2\left(x^2 + y^2\right) + \frac{2q(1-\mu)}{r_1} + \frac{2\mu}{r_2} + \frac{\mu A_2}{r_2^3} - \dot{x}^2 - \dot{y}^2. \tag{1.4.21}$$

The importance of the Jacobi constant is not limited to the concepts of zero velocity surface and zero relative velocity, but it is used for investigation of the regular and

12

chaotic orbits in the RTBP.

1.5 Poincaré maps

In general, algebraic mapping is considered one of the most versatile ways in which a dynamical system in which non–linear equations are involved, can be studied. We can use this method to evaluate the position vector of the particle in the phase space at specified time t, by knowing the position of initial state vector at initial time t_0. This means that the time evolution of the position vector can be described at discrete intervals. The properties and the structures of the dynamical system, which is given by the differential equations, can be represented by using a very simple map.

The properties of complex dynamical systems can be investigated in term of maps by converting the study of a continuous system to the study of an associated discrete system known as Poincaré map. This technique presents three essential features: The dimension reduction, global dynamics, and conceptual clarity. The use of Poincaré map removes at least one variable in the dynamical system, resulting in the investigations and analysis of a lower–dimensional system.

Poincaré surface of sections can highlight the existence of periodic and quasi–periodic orbits. In fact there are two degrees of freedom related to the RTBP in the barycentric synodic frame and one integral constant of motion (Jacobi constant), is given in equation (1.4.21). Therefore the orbits lie on a $3 - dimensional$ subspace $C(x, y, \dot{x}, \dot{y}) = C$ embedded into $4 - dimensional$ phase space. But the Poincaré map of the autonomous dynamical system requires using of a hyperplane or a surface section plane. This plane is usually chosen by fixing one of the coordinates, say $y = 0$, resulting a surface in $3 - dimensions$, which is projected into $2 - dimensional$ plane $(x, \dot{x})$ by specification of another factor [Murray and Dermot (1999)]. We assume that the infinitesimal body started from a point on x–axis, thereby the associated initial value for the perpendicular component of velocity $\dot{y}$ can be evaluated from Jacobi constant in equation (1.4.21) by

$$\dot{y} = \sqrt{n^2 x^2 + \frac{2q(1-\mu)}{r_1} + \frac{2\mu}{r_2} + \frac{\mu A_2}{r_2^3} - \dot{x}^2 - C}. \qquad (1.5.1)$$

The system of equations involved are nonlinear equations and hence obtaining exact solution of the system is difficult. Hence we resort to numerical techniques for solving the equations of motion.

For the construction of surface of sections, the origin of the system under consideration is positioned on the center of mass of the primaries while the smaller primary is assumed to lie on the x–axis to the right side of the more massive primary [Broucke (1968)]. Thus, the origin of this system is positioned on the center of mass of the primaries while the bigger and smaller primaries always lie on the Ox axis at $(-\mu, 0)$ and at $(1 - \mu, 0)$, respectively. Thus, r_1 and r_2 are respectively given by,

$$r_1^2 = (x + \mu)^2 + y^2, \tag{1.5.2}$$

and

$$r_2^2 = (x - 1 + \mu)^2 + y^2. \tag{1.5.3}$$

Using equations (1.4.12), (1.4.13) and (1.4.14), equations of motion can be re written as,

$$\ddot{x} = 2n\dot{y} + n^2 x - \frac{(1-\mu)(x-\mu)q}{r_1^3} - \mu(x - \mu + 1)\left[\frac{1}{r_2^3} + \frac{3A_2}{2r_2^5}\right], \tag{1.5.4}$$

and

$$\ddot{y} = -2n\dot{x} + n^2 y - \frac{(1-\mu)yq}{r_1^3} - \mu y\left[\frac{1}{r_2^3} + \frac{3A_2}{2r_2^5}\right], \tag{1.5.5}$$

which are second order ordinary differential equations. To convert equations (1.5.4) and (1.5.5) in to system of first order differential equations, consider, $y_1 = x$, $y_2 = \dot{x}$, $y_3 = y$ and $y_4 = \dot{y}$. Thus, equations (1.5.4) and (1.5.5) can be written as,

$$\dot{y}_1 = y_2, \tag{1.5.6}$$

$$\dot{y}_2 = 2ny_4 + n^2 y_1 - \frac{(1-\mu)(y_1-\mu)q}{r_1^3} - \mu(y_1 - \mu + 1)\left[\frac{1}{r_2^3} + \frac{3A_2}{2r_2^5}\right], \tag{1.5.7}$$

$$\dot{y}_3 = y_4, \tag{1.5.8}$$

$$\dot{y}_4 = -2ny_2 + n^2 y_3 - \frac{(1-\mu)y_3 q}{r_1^3} - \mu y_3\left[\frac{1}{r_2^3} + \frac{3A_2}{2r_2^5}\right]. \tag{1.5.9}$$

We use Runge–Kutta–Gill fourth order method to integrate the system of first order differential equations. The algorithm for this method is as follows:

14

1. The system of equations are given by

$$\dot{y}_1 = f_1(y_1, y_2, y_3, y_4), \tag{1.5.10}$$
$$\dot{y}_2 = f_2(y_1, y_2, y_3, y_4), \tag{1.5.11}$$
$$\dot{y}_3 = f_3(y_1, y_2, y_3, y_4), \tag{1.5.12}$$
$$\dot{y}_4 = f_4(y_1, y_2, y_3, y_4). \tag{1.5.13}$$

2. Let h be the step size.

3. Evaluate the following quantity:

$$k_1 = h f_1(y_1, y_2, y_3, y_4), \tag{1.5.14}$$
$$l_1 = h f_2(y_1, y_2, y_3, y_4), \tag{1.5.15}$$
$$m_1 = h f_3(y_1, y_2, y_3, y_4), \tag{1.5.16}$$
$$n_1 = h f_4(y_1, y_2, y_3, y_4). \tag{1.5.17}$$

4. Now, update y_1, y_2, y_3 and y_4 as

$$y_1 = y_1 + 0.5k_1, \tag{1.5.18}$$
$$y_2 = y_2 + 0.5l_1, \tag{1.5.19}$$
$$y_3 = y_3 + 0.5m_1, \tag{1.5.20}$$
$$y_4 = y_4 + 0.5n_1. \tag{1.5.21}$$

5. Evaluate the following quantity:

$$k_2 = h f_1(y_1, y_2, y_3, y_4), \tag{1.5.22}$$
$$l_2 = h f_2(y_1, y_2, y_3, y_4), \tag{1.5.23}$$
$$m_2 = h f_3(y_1, y_2, y_3, y_4), \tag{1.5.24}$$
$$n_2 = h f_4(y_1, y_2, y_3, y_4). \tag{1.5.25}$$

6. Now, update y_1, y_2, y_3 and y_4 as

$$y_1 = y_1 + 0.5k_1(-1 + \sqrt{2}) + k_2(1 - 0.5\sqrt{2}), \quad (1.5.26)$$

$$y_2 = y_2 + 0.5l_1(-1 + \sqrt{2}) + l_2(1 - 0.5\sqrt{2}), \quad (1.5.27)$$

$$y_3 = y_3 + 0.5m_1(-1 + \sqrt{2}) + m_2(1 - 0.5\sqrt{2}), \quad (1.5.28)$$

$$y_4 = y_4 + 0.5n_1(-1 + \sqrt{2}) + n_2(1 - 0.5\sqrt{2}). \quad (1.5.29)$$

7. Evaluate the following quantity:

$$k_3 = hf_1(y_1, y_2, y_3, y_4), \quad (1.5.30)$$

$$l_3 = hf_2(y_1, y_2, y_3, y_4), \quad (1.5.31)$$

$$m_3 = hf_3(y_1, y_2, y_3, y_4), \quad (1.5.32)$$

$$n_3 = hf_4(y_1, y_2, y_3, y_4). \quad (1.5.33)$$

8. Now, update y_1, y_2, y_3 and y_4 as

$$y_1 = y_1 - \left[\frac{k_2}{\sqrt{2}} + (1 + \frac{1}{\sqrt{2}})k_3 \right], \quad (1.5.34)$$

$$y_2 = y_2 - \left[\frac{l_2}{\sqrt{2}} + (1 + \frac{1}{\sqrt{2}})l_3 \right], \quad (1.5.35)$$

$$y_3 = y_3 - \left[\frac{m_2}{\sqrt{2}} + (1 + \frac{1}{\sqrt{2}})m_3 \right], \quad (1.5.36)$$

$$y_4 = y_4 - \left[\frac{n_2}{\sqrt{2}} + (1 + \frac{1}{\sqrt{2}})n_3 \right]. \quad (1.5.37)$$

9. Evaluate the following quantity:

$$k_4 = hf_1(y_1, y_2, y_3, y_4), \quad (1.5.38)$$

$$l_4 = hf_2(y_1, y_2, y_3, y_4), \quad (1.5.39)$$

$$m_4 = hf_3(y_1, y_2, y_3, y_4), \quad (1.5.40)$$

$$n_4 = hf_4(y_1, y_2, y_3, y_4). \quad (1.5.41)$$

10. Also, $y_{i,1} = x$, $y_{i,2} = \dot{x}$, $y_{i,3} = y$ and $y_{i,4} = \dot{y}$

11. Then, obtain

$$y_{i+1,1} = y_{i,1} + \frac{1}{6}\left[k_1 + (2 - \sqrt{2})k_2 + (2 + \sqrt{2})k_3 + k_4\right]. \tag{1.5.42}$$

12. Obtain

$$y_{i+1,2} = y_{i,2} + \frac{1}{6}\left[l_1 + (2 - \sqrt{2})l_2 + (2 + \sqrt{2})l_3 + l_4\right]. \tag{1.5.43}$$

13. Obtain

$$y_{i+1,3} = y_{i,3} + \frac{1}{6}\left[m_1 + (2 - \sqrt{2})m_2 + (2 + \sqrt{2})m_3 + m_4\right]. \tag{1.5.44}$$

14. Obtain

$$y_{i+1,4} = y_{i,4} + \frac{1}{6}\left[n_1 + (2 - \sqrt{2})n_2 + (2 + \sqrt{2})n_3 + n_4\right]. \tag{1.5.45}$$

15. $i = i + 1$.

16. Repeat the procedure till desire accuracy is obtained.

Equations (1.5.42) through (1.5.45) give $(x, \dot{x}, y, \dot{y})$ of the secondary body at any time t.

To construct a $2 - dimensional$ Poincaré surface section for a given point $(x, \dot{x})$, the Jacobi constant as well as the hyperplane (surface of section) $y = 0$ can be used. In addition, we assume that the infinitesimal body started from a point on $x-$ axis, thereby the associated initial value for the perpendicular component of velocity $\dot{y}$ can be evaluated from Jacobi constant in equation (1.4.21) by using the relation

$$\dot{y} = \sqrt{n^2x^2 + \frac{2q(1 - \mu)}{r_1} + \frac{2\mu}{r_2} + \frac{\mu A_2}{r_2^3} - \dot{x}^2 - C}. \tag{1.5.46}$$

In this setting, the vector velocity of the infinitesimal body $\vec{V}$ is ruled by

$$\vec{V} = \dot{x}\vec{i} + (\dot{y} + n(x + \mu))\vec{j}, \tag{1.5.47}$$

where $\vec{i}$ and $\vec{j}$ are the unit vectors in the directions of the orthogonal axes for

the rotating frame. With help of equations (1.5.46)and (1.5.47) we can obtain the magnitude of velocity $\vec{V}$, the angular momentum h, the semi–major axis a and the eccentricity e by the following formulae.

$$V = \sqrt{\dot{x}^2 + [\dot{y} + n(x + \mu)]^2}, \tag{1.5.48}$$

$$h = (x + \mu)\left[\dot{y} + n(x + \mu)\right], \tag{1.5.49}$$

$$a = \left[\frac{2}{r_1} - \frac{V^2}{1 - \mu}\right]^{-1}, \tag{1.5.50}$$

$$e = \sqrt{1 - \frac{h^2}{a(1 - \mu)}}. \tag{1.5.51}$$

1.6   Lagrangian points

Lagrangian points or libration points are points at which velocity of secondary body is zero. The RTBP possesses five stationary solutions. Out of these five points, three points are collinear points which are on apse–line, the line joining both primaries. Remaining two points are equilateral points which make equilateral triangles with primaries.
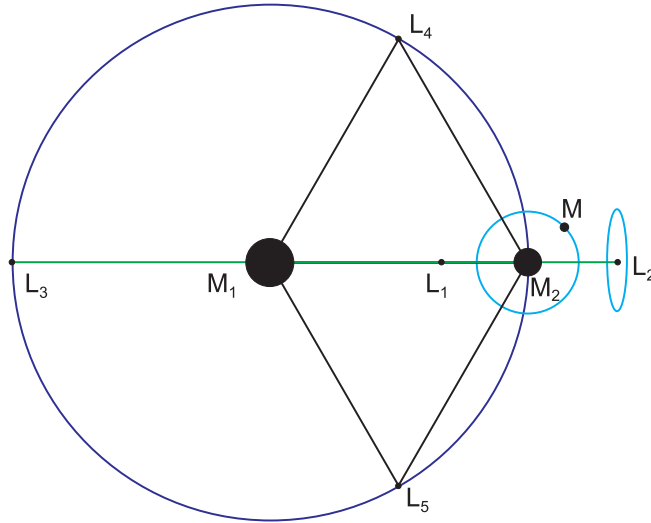

Figure 1.1: Location of Lagrangian points in RTBP.

As shown in Figure 1.1, M_1, M_2 and M are masses of the bigger primary, smaller

primary and secondary body respectively. Three collinear Lagrangian points are denoted by L_1, L_2 and L_3 respectively. L_1 is located between two primaries but very near to smaller primary. In Sun–Earth system, solar wind can be monitored using this point as it reaches early on secondary body located at L_1 than Earth. In Earth–Moon system, to study lunar theory, L_1 plays an important role. L_2 is located right side of the smaller primary. L_3 is located left side of bigger primary. In Sun–Earth system, this point is located behind the Sun. Thus, any secondary body orbiting there can not be visible from Earth. These collinear points are unstable equilibrium points. So, for transferring satellite from orbits around these point to another orbit, these points can be used.

L_4 and L_5 are equilateral triangular Lagrangian points. These two points are stable points. Because of this stability, secondary body like asteroid or dust particles accumulate at that points. For Sun–Jupiter system asteroids are located at these two points. Asteroids which are located at L_4 are known as *Greek camp* and which are located at L_5 are known as *Trojan camp*. Two satellites Tellesto and Callisto of Tethys, which is a Moon of Saturn, are located at L_4 and L_5 respectively.

1.7 Layout of the Thesis

The Thesis is divided into seven chapters in which chapter 1 is introduction which contains motivation and mathematical tools used in the Thesis. This chapter concludes with the summary of subsequent chapters.

Chapter 2 deals with evolution of the periodic orbits, quasi periodic orbits and chaotic orbits in the photo gravitational Sun-Saturn system incorporating actual oblateness of Saturn in the planar circular restricted three body problem. The effect of the perturbation due to solar radiation pressure for various values of Jacobi constant C on various geometric parameters like location, eccentricity, diameter and semi major axis of the Sun centered and Saturn centered periodic orbits is investigated using Poincare surface of section method.

It is observed that the introduction of solar radiation pressure decreases the admissible range of Jacobi constant C, and as the value of C decreases the number of

islands decreases and consequently the number of periodic and quasi periodic orbits decreases. Further, the periodic orbits around Saturn and Sun moves towards Sun on decreasing perturbation due to solar radiation pressure q for a fixed value of Jacobi constant C. It is also observed that due to solar radiation pressure, semi major axis and eccentricity of Sun centered periodic orbit decrease.

Chapter 3 includes analysis of the periodic orbits of f family (simply symmetric retrograde periodic orbits) and the regions of quasi-periodic motion around Saturn in the photo gravitational Sun-Saturn system in the framework of planar circular restricted three-body problem with oblateness. It is observed that radiation pressure has significant influence on evolution of family f of periodic orbit. As radiation pressure increases the admissible value of C decreases and periodic orbit shifts towards Saturn. Also the geometric parameters of the orbits such as diameter, eccentricity and semi major axis decrease. An increment in C increases the semi-major axis of f family of periodic orbits while the eccentricity decreases up to certain value of C and then shows a sudden increase in its value. Diameters of these periodic orbits decrease slowly, but after certain value of C, there is a sudden decrement in value of diameter of periodic orbits. It is also observed that as solar radiation pressure decreases, the location of periodic orbits at both separatrices moves towards Saturn. Also, as q moves towards 1, the value of Jacobi constant corresponding to both separatrices moves towards 3. Further, the difference between corresponding Jacobi constant decreases as q decreases up to 0.9845 and then increases slightly. It can be seen that the difference between location of two periodic orbits at both separatrices decreases as q drops to the value 0.9845 and then slightly increases. Thus, as the perturbation due to solar radiation pressure decreases, the two separatrices come closer to each other and also come closer to Saturn. It is found that the eccentricity and semi major axis of periodic orbits at both separatrices are increased by perturbation due to solar radiation pressure. The evolution of the family of periodic orbits can be divided into three stages separated by two separatrices. In other words, there is a change in the way the quasi-periodic orbits oscillate around the periodic orbits before and after these separatrices. Family f can be used for patching of trajectory of satellite, that is, joining of two or more orbits to obtain a trajectory.

In Chapter 4 we have investigated the effect of oblateness on the position, shape and

size of closed periodic orbit with loops varying from 1 to 5 for Sun-Mars and Sun-Earth systems, respectively. It is found that for given number of loops and given C, as oblateness increases, location of periodic orbit moves towards Sun. For given C and given oblateness, as number of loops increases, location of periodic orbits shifts towards Sun. Also, for given value of oblateness and given number of loops, as C decreases, location of periodic orbit moves towards Sun. Also, period of the orbit increases as number of loops increases. It is also observed that single-loop orbit is closest to second primary body. Further, as number of loops decreases, width of the orbit increases. The distance of closest approach of the infinitesimal particle from the smaller primary increases with oblateness and number of loops for a given C. Thus, the present analysis of the two systems- Sun-Mars and Sun-Earth systems using PSS technique reveals that A_2 and C has substantial effect on the position, shape and size of the orbit. The PSS together with regression analysis will help one to locate the position of the periodic orbit with less effort, using the predicted positions from the analysis.

It can be observed that for given oblateness and given number of loops, as Jacobi constant decreases, initial velocity of infinitesimal particle (spacecraft) and distance of spacecraft from second primary increase and distance of spacecraft from first primary body decreases. For given Jacobi constant and given number of loops, as oblateness increases, initial velocity increases and distance of spacecraft from second primary increases and the distance of spacecraft from first primary decreases. Thus, the effects of Jacobi constant C and oblateness coefficient A_2 are opposite in nature. For given value of oblateness coefficient and Jacobi constant, as number of loops increases, distance of spacecraft from second primary increases and distance of spacecraft from first primary decreases where as initial velocity of spacecraft decreases from one–loop orbit to three–loops orbit and then increases from three–loops orbit to five-loops orbit. It is further observed that for Sun–Mars system, single–loop orbit for $A_2 = 0.00001$ and $C = 2.96$ is closest to Mars and this distance is 3.886×10^7 km. Whereas, for Sun-Earth system, single-loop orbit for $A_2 = 0.00001$ and $C = 2.96$ is closest to Earth and this distance is 2.542×10^7 km. Since stability of this class of periodic orbits is very low, it can be used for designing low-energy trajectory design for space mission.

21

Chapter 5 is devoted to the study of the effect of solar radiation pressure on the position, shape and size of closed periodic orbit with loops varying from 1 to 5 for Sun–Mars and Sun–Earth systems, respectively. A noticeable difference observed in both the systems is that for $C = 2.96$, $q = 0.995$, single–loop periodic orbit, for $C = 2.96, q = 0.99$, two–loops orbit, for $C = 2.96, q = 0.9845$, three–loops periodic orbit does not exist for Sun–Earth system whereas it exist for Sun–Mars system. The distance of closest approach of the infinitesimal particle from the smaller primary decreases with increase in solar radiation pressure from 1 to 0.9845 and distance between smaller primary and infinitesimal particle increases as number of loops increases for a given C and q. It is found that the eccentricity decreases as number of loops increases. For a given number of loops, the eccentricity is found to decrease as solar radiation pressure increases from 1 to 0.9845. Thus, the present analysis of the two systems - Sun–Mars and Sun–Earth systems–using PSS technique reveals that q and C have substantial effect on the position, shape and size of the orbit.

It can be observed that for given solar radiation pressure and given number of loops, as Jacobi constant decreases, initial velocity of infinitesimal particle and distance of infinitesimal particle from second primary increase and distance of infinitesimal particle from first primary body decreases.

For given Jacobi constant and given number of loops, as solar radiation pressure increases from 1 to 0.9845, initial velocity decreases and distance of infinitesimal particle from second primary decreases. So, distance of infinitesimal particle from first primary increases. Thus, the effect of Jacobi constant C and solar radiation pressure q is opposite in nature. For given value of solar radiation pressure q and Jacobi constant, as number of loops increases, distance of infinitesimal particle from second primary increases and distance of infinitesimal particle from first primary decreases. It is further observed that for Sun–Mars system, single–loop orbit for $q = 0.995$ and $C = 2.96$ is closest to Mars and this distance is 7.521×10^5 km, whereas for Sun–Earth system, single–loop orbit for $q = 0.99$ and $C = 2.95$ is closest to Earth and this distance is 7.535×10^5 km. Since these orbits can be used for designing low–energy space mission. Hence detailed study is presented in this chapter. Stability analysis of this family of orbit indicates that these orbits having smaller stability region in comparison to f family orbit. So, these orbits can be used as a transfer trajectory as less amount of fuel required for transferring of satellite from one orbit to another orbit. For each pair of (q, C), there are two separatrices

exist where stability of periodic orbit becomes zero.

In Chapter 6 , we investigate exterior and interior first, third and fifth order resonances in the photo–gravitational restricted three–body problem by numerical methods for the Sun-Earth and the Sun–Mars systems considering the Sun as a radiating body and Earth or Mars as an oblate spheroid. In this context, the first order exterior and interior resonant orbits are analyzed with and without perturbation for $C = 2.93$. It is observed that for the given order of resonance, period of the orbit is increased by exactly 6 or 7 units as number of loops is increased by one because period of the second primary (Earth or Mars) body's orbit is 6.282714 units. It is noticed that for the external resonance as the number of loops increases, location of the periodic orbit moves towards the Sun whereas for the internal resonance, as the number of loops increases, location of the periodic orbit moves away from the Sun. Also, location of exterior or interior first order resonant orbits moves away from the Sun as perturbation included. While from location of orbits, we can conclude that exterior resonance orbits with and without perturbation are nearer to the Earth whereas interior resonant orbits are nearer to the Sun. So, for the orbit having same number of loops, location of interior resonant orbit is nearer to the Sun in comparison to the exterior resonant orbit.

Eccentricity of the periodic orbit decreases as number of loops increases for both interior and exterior resonance in both perturbed and unperturbed cases. Also, for the orbit having same number of loops, eccentricity of interior resonant orbit is more in comparison to exterior resonant orbit. We also observe that for the given order of resonance as perturbation increases eccentricity of the periodic orbit decreases. Furthermore, we study the evolution of three loops orbit for interior first order resonance by changing value of Jacobi constant C. As value of C increases, size of the loop reduces, and hence the shape of the orbit changes and finally it becomes circle. Thus, as C increases, eccentricity of the periodic orbit decreases and location of the periodic orbit moves towards the second primary body, namely, Earth or Mars. Regard to the location of third and fifth order resonant orbits for $C = 2.93, q = 0.9845$ and $A_2 = 0.0001$ shifts towards the second primary as the number of loops increases. Third and fifth order resonant orbits are divided in to two families. Orbits of Family I are around the first primary only, whereas, orbits

of Family II are around both the primaries in which one of the loops of the orbit is around the second primary body, namely, Earth or Mars. It is concluded that for the given number of loops, as order of resonance increases location of periodic orbits moves towards the Sun. Also, eccentricity of the orbit decreases as the number of loops increases, and eccentricity of Family I orbit is higher than Family II orbit for the given order of resonance. It can be observed that for the given number of loops, as order of resonance increases eccentricity increases. Period of the first, third and fifth order resonance orbit increases as the number of loops increases. Also, period of Family II orbit is higher than the Family I orbit for the given order of resonance. Further we notice that for the given number of loops, as order of resonance increases period decreases, which is obvious.

Chapter 7 includes analysis of interior seventh, ninth and eleventh order resonances in the restricted three-body problem for the Sun-Earth and the Sun-Mars systems by considering the Sun as a radiating body and both the Earth and Mars as oblate spheroid. It is observed that for the given order of resonance, period of the orbit is increased by exactly 6 or 7 units as number of loops is increased by one because period of the infinitesimal bodys orbit is 6.2827 units. It is concluded that for the internal resonance, as the number of loops increases, location of the periodic orbit moves away from the Sun. Eccentricity of the periodic orbit decreases as number of loops increases for interior resonance in perturbed case. For the given order of resonance as perturbation increases eccentricity of the periodic orbit decreases. It is concluded that for the given number of loops, as order of resonance increases location of periodic orbits moves towards the Sun. Also, eccentricity of the orbit decreases as the number of loops increases. It can be observed that for the given number of loops, as order of resonance increases eccentricity increases. Period of the seventh, ninth and eleventh order resonance orbit increases as the number of loops increases. It can be observed that for the given number of loops, as order of resonance increases period decreases, which is obvious.

Chapter 7 is followed by Appendix– A, list of publications and references used during the course of research are listed at the end in alphabetic order.